

Electronic Supplementary Information (ESI) for ChemComm.
This journal is © The Royal Society of Chemistry 2021

Electronic Supplementary Information (ESI) for

Spatially isolated CoN_x quantum dots on carbon nanotubes enable a robust radical-free Fenton-like process

Jia-Cheng E. Yang,^a Min-Ping Zhu,^{ab} Darren Delai Sun^c Ming-Lai Fu,^{*ad} and Yu-Ming Zheng,^{*ab}

^a CAS Key Laboratory of Urban Pollutant Conversion, Institute of Urban Environment (IUE), Chinese Academy of Sciences (CAS), No. 1799, Jimei Avenue, Xiamen 361021, China.

^b University of Chinese Academy of Sciences (UCAS), No. 19(A), Yuquan Road, Shijingshan District, Beijing 100049, China.

^c School of Civil and Environmental Engineering, Nanyang Technological University, 639798, Singapore.

^d Xiamen Key Laboratory of Municipal and Industrial Solid Waste Utilization and Pollution Control, College of Civil Engineering, Huaqiao University, Xiamen 361020, China.

* Correspondence should be addressed to Professor Yu-Ming Zheng (ymzheng@iue.ac.cn) and Professor Ming-Lai Fu (mlfu@iue.ac.cn, mlfu@hqu.edu.cn).

Table of Contents

S1 Experiment section	S3
S1.1 Reagents & Materials	S3
S1.2 Synthesis of spatially isolated CoN _x quantum dots on CNTs (CoN _x -CNTs)	S3
S1.3 Synthesis of β-MnO ₂ nanorods.....	S3
S1.4 Materials characterizations.....	S3
S1.5 Degradation experiments.....	S4
S1.6 Detection of reactive oxygen species	S4
S1.7 Degradation of AO7 in real water matrix condition	S5
S1.8 Analysis methods	S5
S1.9 Product identification and toxicity assessment.....	S5
S2 Figures and Tables	S6
Fig. S1.	S6
Fig. S2.	S7
Fig. S3.	S8
Fig. S4.	S9
Fig. S5.	S10
Table S1	S11
Table S2	S13
Table S3	S13
Table S4	S14
Author Contributions	S15
Notes and references	S15

S1. Experiment section

S1.1 Reagents & Materials

Commercial multiwall carbon nanotubes (CNTs) (Purity: 95%, diameter: 10 – 20 nm, length: 10 – 30 μm) were purchased from Chengdu Organic Chemicals Co. Ltd., China. The PMS was generated from commercial Oxone[®] (CAS: 70693-62-8, $\text{KHSO}_5 \cdot 0.5\text{KHSO}_4 \cdot 0.5\text{K}_2\text{SO}_4$, from Aladdin Co. Ltd., China). Commercial nano cobalt oxide (Co_3O_4 , CAS: 1308-06-1, 100 nm, 99.5% metal basis, Lot# A1706043) and commercial nano Fe_3O_4 (Fe_3O_4 , CAS: 1317-61-9, 20 nm, Lot# A1607150) were supplied by Aladdin Co. Ltd., China. Formamide and $\text{Co}(\text{NO}_3)_2 \cdot 6\text{H}_2\text{O}$ were from Sinopharm, Shanghai, China. Other chemicals were used as received without further purification. Deionized water (18.25 M Ω) was used to prepare all the solutions in this study.

S1.2 Synthesis of spatially isolated CoN_x quantum dots on CNTs ($\text{CoN}_x\text{-CNTs}$)

The catalysts of $\text{CoN}_x\text{-CNTs}$ were prepared by a reported method of formamide (FA)-based solvothermal reaction with slight modification [1]. In detail, 0.3 mmol of $\text{Co}(\text{NO}_3)_2 \cdot 6\text{H}_2\text{O}$ (87.3 mg) was firstly added into 30 mL of FA. After stirring for 30 min, 100 mg of commercial CNTs (as received) was dispersed into the solution. The obtained solution was then transferred into a 50-mL Teflon autoclave, followed by heating it at 170 $^\circ\text{C}$ for 12 h. After cooling to room temperature, the black suspension was filtered and re-dispersed in ethanol. After filtration, the sample was washed with deionized water 3 times, followed by a freeze-drying procedure overnight. In addition, identical procedures without $\text{Co}(\text{NO}_3)_2 \cdot 6\text{H}_2\text{O}$ or CNTs were repeated to prepare N-doped CNTs and CoN_x for comparison. The average mass of CoN_x nano-clusters in-situ formed on CNTs (100 mg) is more than 21.6 mg, while the average mass of resultant CoN_x without the support of CNTs is only about 5.5 mg, suggesting the positive role of CNTs in promoting the formation of more CoN_x nano-clusters.

S1.3 Synthesis of $\beta\text{-MnO}_2$ nanorods

The $\beta\text{-MnO}_2$ nanorods were prepared by a facial hydrothermal process with the following steps: 4 mmol of $(\text{NH}_4)_2\text{S}_2\text{O}_8$ and 4 mmol of $\text{MnSO}_4 \cdot \text{H}_2\text{O}$ were firstly mixed in 160 mL of deionized water to form a homogeneous solution. The solution was then transferred into a 200-mL Teflon autoclave reactor and heated at 140 $^\circ\text{C}$ for 12 h. After cooling to the room temperature, the aqueous suspension was filtered and re-dispersed in water, followed by a filtration step. The filtration-washing step was repeated 3 times to remove residues. The obtain sample was dried at 100 $^\circ\text{C}$ overnight then ground on an agate mortar for further use.

S1.4 Materials characterizations

X-ray diffraction (XRD) spectra of CNTs, N-CNTs and $\text{CoN}_x\text{-CNTs}$ were obtained on an X'Pert PRO diffractometer (PANalytical, Holland, $\text{Cu } K_\alpha$, $\lambda = 0.15406 \text{ nm}$) with 40 KV accelerating voltage and 40 mA current. The data were collected from 5 $^\circ$ to 80 $^\circ$ at a scan speed of 0.6 $^\circ$ /min. High-resolution transmission electron microscopy (HRTEM, operated at 200 kV) images were recorded using a JEOL 2100 high-resolution transmission electron microscope. The aberration-corrected high-angle annular darkfield scanning transmission electron microscope (HAADF-STEM) and element mapping images of $\text{CoN}_x\text{-CNTs}$ were recorded on an instrument of FEI Titan Themis 60-300 with a spherical aberration corrector (operated at 200 kV). The element information of CNTs, N-CNTs and $\text{CoN}_x\text{-CNTs}$ was examined by K-Alpha X-ray photoelectron spectroscopy (XPS) system, (X-ray Source: Mg).

The linear sweep voltammetry (LSV) experiments were performed in the solution of 0.5 M Na_2SO_4 at a scan rate of 5 mV/s. Prior to LSV tests, the working electrode was firstly prepared by immobilizing the black ink containing 500 μg $\text{CoN}_x\text{-CNTs}$ onto the 1 \times 1 cm^2 conductive carbon paper (CCP), followed by drying them naturally. The LSV measurements were carried out in a standard three-electrode system (CHI

660D, Shanghai Chenhua, China) with the working electrode of CoN_x-CNTs-containing CCP, the reference electrode of Ag/AgCl and the counter electrode of platinum plate. All potentials reported in this work were referenced to a reversible hydrogen electrode (RHE). The data were obtained at room temperature and reported between -0.1 and 0.45 V vs RHE. The concentrations of PMS and AO7 used for LSV tests are 0.2 g L⁻¹ and 10 mg L⁻¹, respectively.

S1.5 Degradation experiments

The activities of CoN_x-CNTs and other catalysts in PMS activation were tested by using acid orange VII (AO7) as a model recalcitrant organic contaminant (ROC). Batch experiments were conducted in 50 mL beakers containing 40 mL of AO7 solution (10 mg L⁻¹) with magnetic stirring (400 rpm) at room temperature (301 ± 2 K). Firstly, 1 mg of CoN_x-CNTs was dispersed with the help of ultrasonic for 30 s. The solution was first stirred for at least 5 mins by utilizing a magnetic stirring apparatus before adding PMS solution (80 µL, 100 g L⁻¹) to initiate the degradation reaction. At the predetermined time intervals, 600 µL of samples were withdrawn and quenched with 50 µL of 0.5 M S₂O₃²⁻ and 150 µL of ethanol. The initial pH of AO7 solution was adjusted with dilute H₂SO₄ and/or NaOH solutions in advance. The effects of initial pH (3 – 10.6) and co-anions (AO7 containing 10 mM of NaCl, NaNO₃, NaHCO₃, Na₂SO₄ or Na₃PO₄) on the reactivity of CoN_x-CNTs toward PMS activation were studied. CoN_x-CNTs were replaced with N-CNTs (1 mg), CNTs (2 mg), cnCo₃O₄ (6 mg), cnFe₃O₄ (2 mg) or β-MnO₂(2 mg) to conduct the comparison study with the above procedures.

Following the above procedures, the degradation of other ROCs (10 mg L⁻¹), such as phenol, 2-chlorophenol (2-CP), butyl paraben (BuP) and bisphenol A (BPA), were also studied to examine the reactivity of CoN_x-CNTs (1.5 mg) toward PMS (0.2 g L⁻¹) activation.

The reusability of CoN_x-CNTs were carried out as follows: I) 1.5 mg of CoN_x-CNTs was firstly dispersed in 40 mL of AO7 solution (10 mg L⁻¹) with the help of ultrasonic for 30 s. Then the solution was stirred for at least 5 mins (400 rpm) before adding PMS solution (80 µL, 100 g L⁻¹) to initiate the degradation reaction at room temperature (293 K). At the reaction of 5 min, 600 µL of samples were withdrawn and quenched with 50 µL of 0.5 M S₂O₃²⁻ and 150 µL of ethanol. II) The spent CoN_x-CNTs were harvested by centrifugation (6000 g, 5 min) without any additional washing steps, and directly used for the second removal of AO7 under the above identical conditions. III) The CoN_x-CNTs after second use were firstly harvested by centrifugation (6000 g, 5 min). The collected solid samples were dispersed in deionized water under ultrasonic and harvested by centrifugation (6000 g, 8 min). After the washing step was repeated two times, the solid samples were dried at 65 °C. Lastly, identical steps were employed to remove AO7 for the third use of CoN_x-CNTs. Considering the remarkably reduced removal rate of AO7, we did not carry out the next reuse of CoN_x-CNTs.

S1.6 Detection of reactive oxygen species

The possible reactive species in the CoN_x-CNTs/PMS system were firstly identified by quenching tests. The AO7 solutions with a predetermined concentration of ethanol (EtOH, 1 M), *tert*-butyl alcohol (TBA, 1 M), *p*-benzoquinone (BQ, 2 mM) or L-histidine (HD, 2 mM and 20 mM) were firstly prepared. Before repeating the identical procedures mentioned in S1.5 to examine the effects of scavengers on the reactivity of CoN_x-CNTs toward PMS activation with respect to the degradation of AO7. The reactive oxygen species (ROS) generated in the CoN_x-CNTs/PMS system were detected by electron paramagnetic resonance (EPR) (JEOL-FA200). 5,5-dimethyl-1-pyrroline N-oxide (DMPO) and 2,2,6,6-tetramethyl-4-piperidone (TEMP) were used as the spin trapping reagents with the following operating conditions: Sweep, 1 min; center field, 322.989 mT; sweep width, 5 × 1 mT; microwave frequency, 9067.390 – 9068.987 MHz; microwave power, 0.998 mW; modulation frequency, 100 kHz; modulation width, ± 0.5 × 0.1 mT; modulation amplitude, 2.0 × 1; time, 0.03 s. Other reaction conditions for ROS detection are:

[DMPO] = 323 mM, [TEMP] = 197 mM, [CoN_x-CNTs] = 0.025 g/L, [PMS] = 0.2 g/L, pH = 7.0.

S1.7 Degradation of AO7 in real water matrix condition

Firstly, tap water and river water in our institute were used to prepare the simulated dye wastewater. After which 1 mg of CoN_x-CNTs were used to activate PMS (0.2 g L⁻¹) oxidise AO7 (10 mg L⁻¹) in the simulated wastewater with the identical procedures mentioned in S1.5. Since the initial pH of tap water and river water was around neutral condition, we did not further adjust the initial solution pH and placed them as they are.

S1.8 Analysis methods

The concentration of AO7 was determined by UV-Vis spectrophotometry method at 483 nm (Evolution 300, Thermo, USA). The before and after reactions pH values of solutions were measured with a pH meter. A high-performance liquid chromatograph (HPLC, Agilent 1260) equipped with a diode array detector and an Eclipse C18 column (5 μm, 4.6 mm × 250 mm, Agilent) at 30 °C was employed to determine the concentrations of phenol, 2-CP, BuP and BPA. Their analytical conditions, like mobile phases, detection wavelengths and flow rates, were summarized in Table S3. The concentrations of cobalt ions released from CoN_x-CNTs were determined by inductively coupled plasmaatomic emission spectrometry (ICP-AES, Optima 7000DV, PerkinElmer, USA).

S1.9 Product identification and toxicity assessment

The degradation products of AO7 were identified by ultra-high performance liquid chromatograph with a Q Exactive mass spectrometer (MS) system (Ultimate 3000 UPLC, Thermo scientific). The separation was performed with a Hypersil GOLD column (2.1 × 100 mm, 3 μm; Thermo Scientific). The flow rate and detector temperature were set to 0.25 mL/min and 298 K, respectively. The mobile phase was a gradient of acetonitrile (A) and water (B), both with 0.1% formic acid. The gradient elution conditions were optimized as follows: 5% A (0 – 3 min), linear gradient from 5 to 80% A (3 – 12 min), 80% A (12 – 14 min), linear gradient from 80 to 5% A (14 – 14.1 min), and 5% A (14.1 – 20 min). Both positive and negative modes with a mass range from 50 – 750 m/z were used to detect the products. The optimized MS conditions are summarized as follows: spray voltage (3200 V), capillary temperature (300 °C), sheath gas (40 psi), aux gas (15 psi), max spray current (100 uA), probe heater temperature (350 °C). For simplicity, the final product with a molecular weight of *w* was marked as P_w. In the light of the peak area, the relative proportion of each product (*f*_{P_w}, %) was also calculated to probe the main degradation pathways of IBU by a given oxidation system (see Table S4).

The values of development toxicity and *Oral rat* LD50 for parent AO7 and each degradation product were calculated using the Toxicity Estimation Software Tool (T.E.S.T). The results were summarized in Table S4. The normalized total toxicity value of all products (*T*_{NT,All}) was calculated as following:

$$T_{NT,All} = \sum_0^{All\ products} (T_{st,Pw} * f_{Pw})$$

where *T*_{st,P_w} is a special toxicity value for the product of P_w (e.g., the developmental toxicity value of P202 to humans or animals is 0.51), while *f*_{P_w} (%) is the relative proportion for the product of P_w (e.g., 84.88% for P202). Based on these rules, the theoretical normalized total developmental toxicity of all products for the degradation of AO7 is 0.53, while the normalized total *Oral rat* LD50 is 2595.20 mg/kg.

S2. Figures and Tables

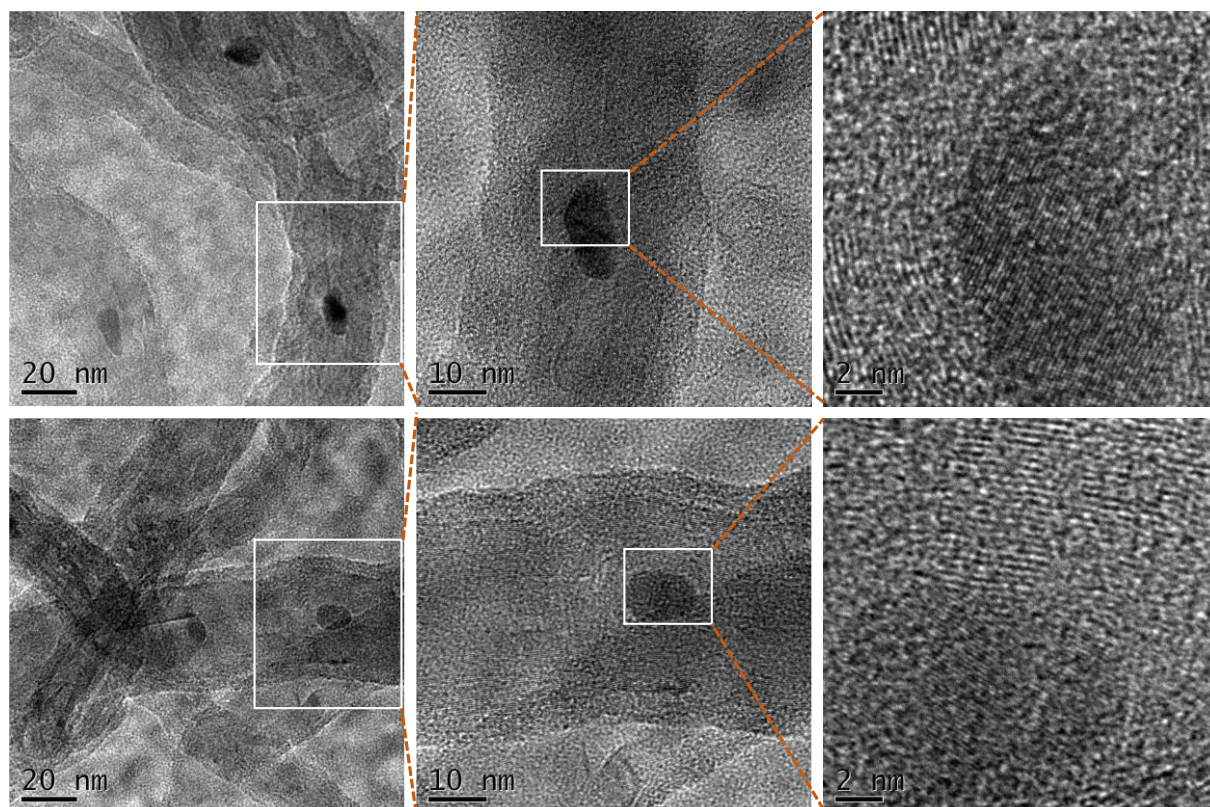


Fig. S1. Typical HR-TEM images of Co_N-CNTs.

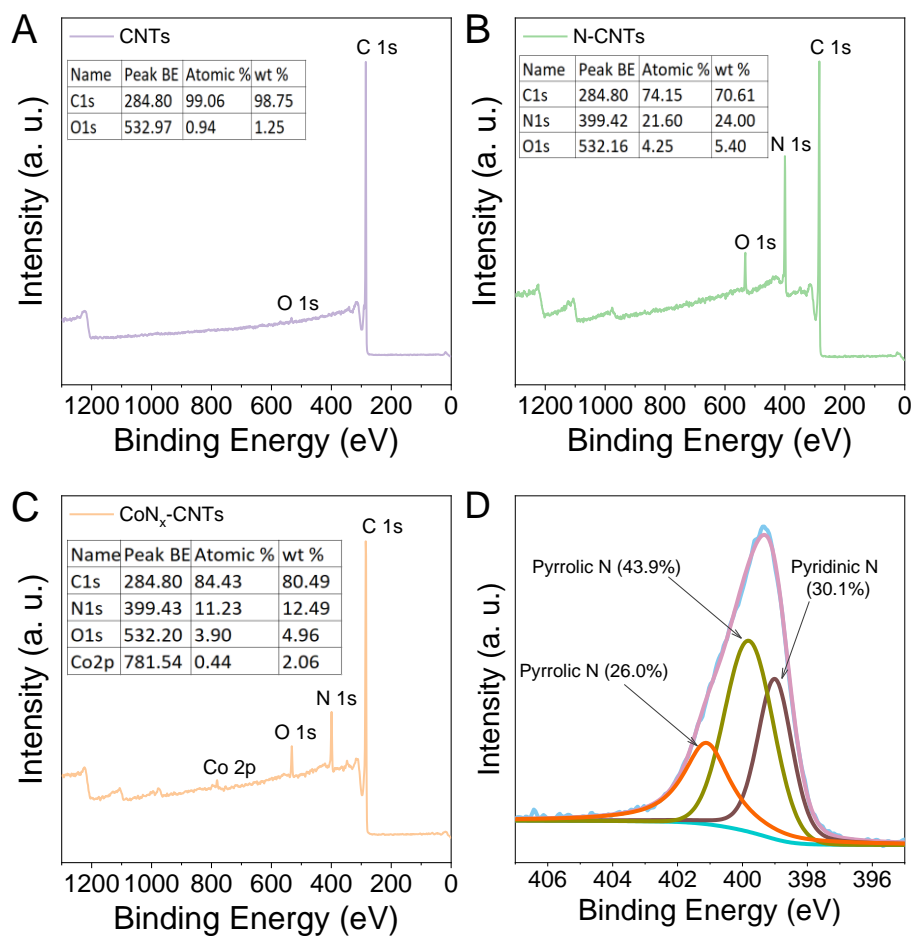


Fig. S2. XPS survey of CNTs (A), N-CNTs (B) and CoN_x-CNTs (C), and high-resolution N 1s XPS spectrum of N-CNTs (D).

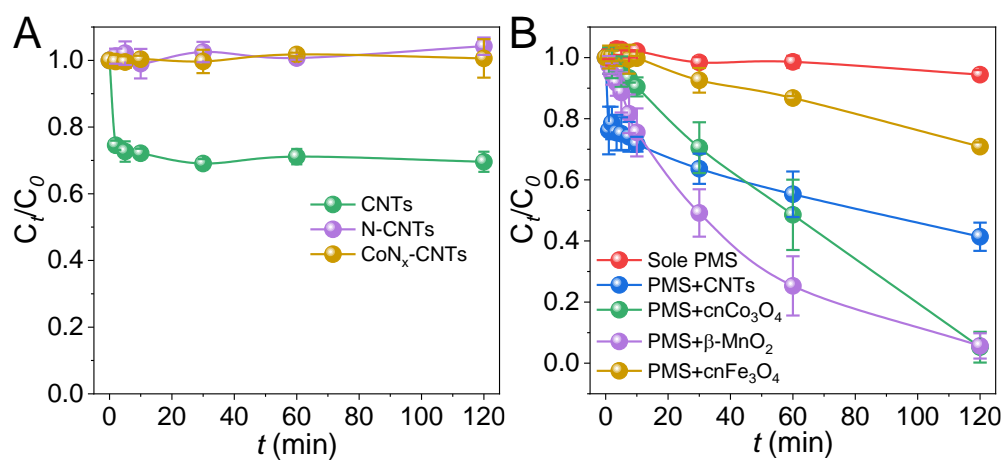


Fig. S3. The adsorption capacity of CNTs, N-CNTs and CoN_x-CNTs toward AO7 (A). The comparison on the catalytic activities of CNTs, cn-Co₃O₄, β-MnO₂ and cn-Fe₃O₄ with respect to the activation of PMS and degradation of AO7(B).

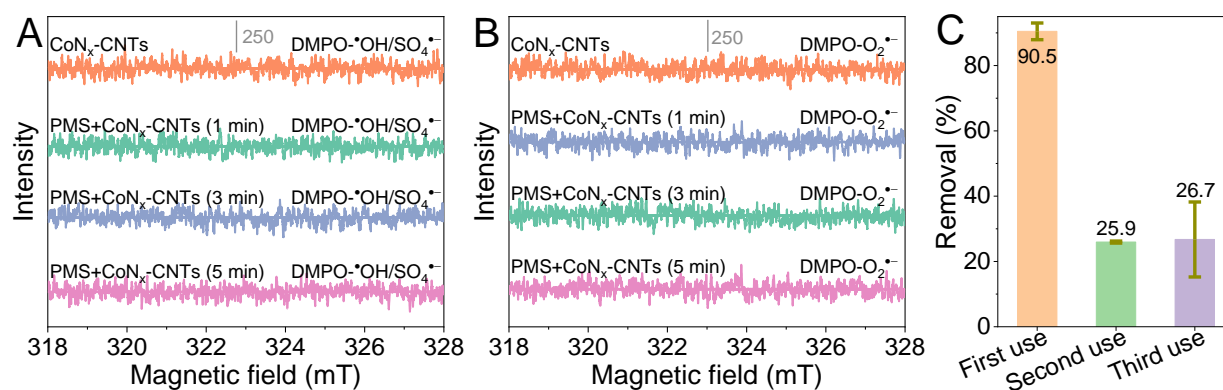


Fig. S4. EPR spectra of DMPO trapped radical adducts in the PMS/CoN_x-CNTs system (B for the trapped $\cdot\text{OH}/\text{SO}_4^{\cdot-}$ adducts, while C for the trapped $\text{O}_2^{\cdot-}$ adducts). The reusability of CoN_x-CNTs toward PMS activation for AO7 removal (A).

Fig. S4A and S4B shows that neither DMPO- $\cdot\text{OH}/\text{SO}_4^{\cdot-}$ nor DMPO- $\text{O}_2^{\cdot-}$ adducts were detected in the EPR spectra, suggesting the absence of radicals in the CoN_x-CNTs/PMS system. This observation agrees with the results of quenching experiments and LSV characterization (Fig. 4A and 4C).

As shown in Fig. S4C, compared with the first use, the spent CoN_x-CNTs in the second use cannot maintain their initial activity toward the activation of PMS for the degradation of removal. Moreover, even though the spent CoN_x-CNTs was cleaned and dried, their activity still cannot be recovered in the third use. This finding is similar to the documented activation of PMS with N-doped CNTs and graphene in previous work [2, 3]. We think this phenomenon is attributed to two facts: I) The residual degradation products on the active sites of CoN_x-CNTs deteriorated their catalytic performance. II) The high-valent cobalt-oxo species or CoN_x-OOSO₃ were completely consumed, probably resulting in the formation of other cobalt-based species with low activity. So, the reusability of CoN_x-CNTs was low and further regeneration search is being designed and carried out.

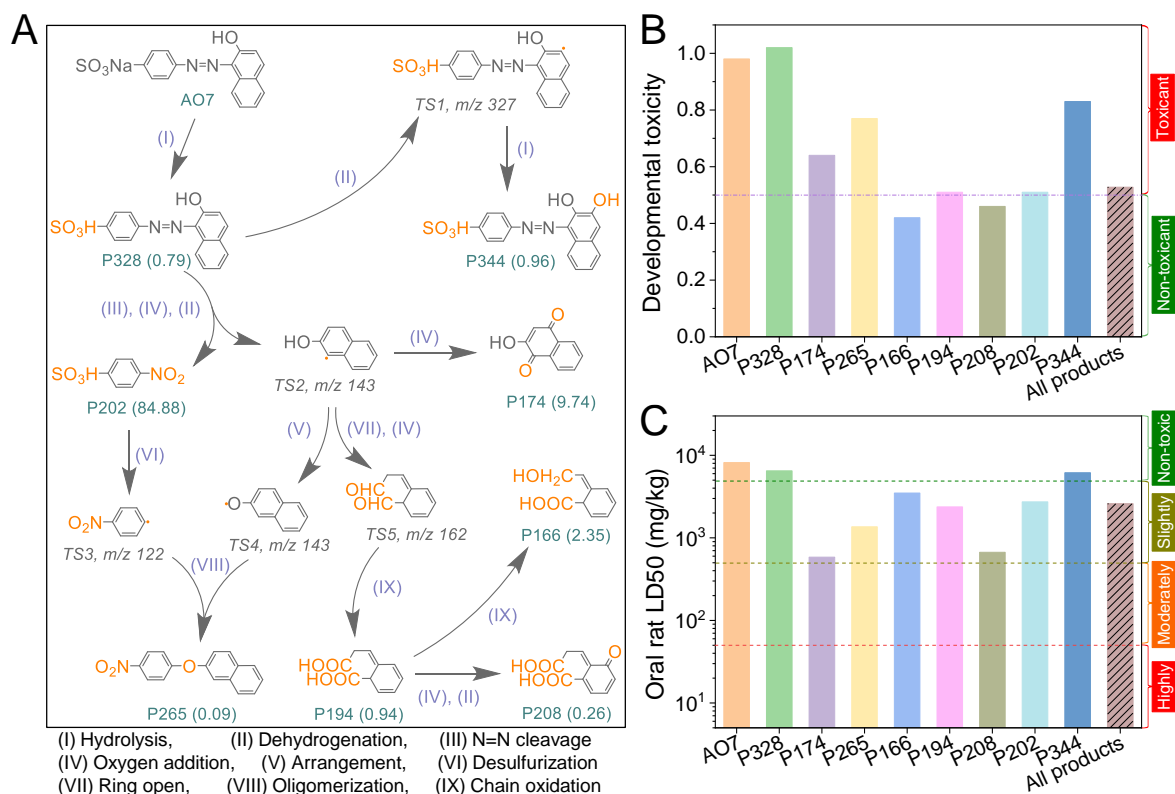


Fig. S5. The proposed pathways for the degradation of AO7 by CoN_x-CNTs/PMS (A), the theoretical developmental toxicity (B) and the *Oral rat* LD50 (C) of parent AO7 (in the form of C₁₆H₁₁N₂O₄S⁻), its single degradation product and all products.

As shown in Fig. S5A and Table S4, P202 is the degradation product for the degradation of AO7 by CoN_x-CNTs/PMS. Hydrolysis, N=N cleavage and oxygen addition are the main pathways for the formation of P202. The oxygen addition on the radical cation TS2 (induced by dissolved oxygen and singlet oxygen) can result in the second most important product of P174. Some insignificant products, like P344, P328, P265, P208 and P194, can also be formed via the pathways shown in Fig. S5A.

Besides P328, the rest of products have lower developmental toxicity than AO7, and the theoretical normalized total developmental toxicity of all products is 0.53, much lower than that of AO7 (0.98) (Fig. S5B). This finding suggests the oxidation degradation of AO7 by CoN_x-CNTs/PMS helps to reduce the developmental toxicity of AO7 to humans and animals. Fig. S5C implies that the higher the *Oral rat* LD50 value is, the lower the toxicity of the product is. Unfortunately, all products have lower *Oral rat* LD50 values than AO7 (8168.36 mg/kg), and the normalized total *Oral rat* LD50 is 2595.20 mg/kg, implying that the degradation of AO7 by CoN_x-CNTs/PMS slightly increased the toxicity to the rat. These results suggest a necessity of systematically studying the toxicity risks of radical-free and selective oxidation for aqueous environmental remediation [4].

Table S1. Summary on the synthesis methods of newly catalysts and their catalytic performance toward PMS activation for the degradation of organics.

Catalysts (g L ⁻¹)	Materials	Synthesis methods	PMS concentration	Pollutants [‡] (mg L ⁻¹)	Degradation process	Initial pH	k (min ⁻¹)	K _d (min ⁻¹ (g L ⁻¹) ⁻¹)	Refs
CoN _x -CNTs (0.025)	Co(NO ₃) ₂ ·6H ₂ O, formamide, CNTs	Solvothermal reaction (170 °C 12 h)	0.20 g L ⁻¹ (0.65 mM)	AO7 (28.54 μM, 10 mg L ⁻¹)	¹ O ₂ , cobalt-HSO ₅ complex, cobalt-oxo-based degradation	7.00	9.29E-01	37.14	This work
CoN _x -CNTs (0.0375)	Co(NO ₃) ₂ ·6H ₂ O, formamide, CNTs	Solvothermal reaction (170 °C 12 h)	0.20 g L ⁻¹ (0.65 mM)	2-CP (77.78 μM, 10 mg L ⁻¹)	¹ O ₂ , cobalt-HSO ₅ complex, cobalt-oxo-based degradation	7.00	7.78E-01	20.80	This work
Co-SA (0.2)	Co(NO ₃) ₂ ·6H ₂ O, Zn(NO ₃) ₂ ·6H ₂ O, 2-methylimidazole, 1-methylimidazole, methanol	Precursor synthesis, pyrolysis (900 °C 2 h, Ar), acid washing (80 °C 4 h)	0.3 g L ⁻¹ (0.976 mM)	CIP (60.36 μM, 20 mg L ⁻¹)	¹ O ₂ -based degradation	7.00	1.40E-01	0.70	[5]
Fe1/CN (0.5)	Melamine, cyanuric acid, Fe(NO ₃) ₃ ·H ₂ O, Oxalic acid dihydrate	Precursor synthesis (80 °C), pyrolysis (600 °C 4 h, Ar)	20 mM	4-CP (100 μM, 12.86 mg/L)	¹ O ₂ -based degradation	-	1.43E+00	2.86	[6]
Fe-SAC (0.2)	2-methylimidazole, methanol, Zn(NO ₃) ₂ ·6H ₂ O, Fe(acac) ₃ , 1,10-phenanthroline, ethanol	Carbon support synthesis (1100 °C 2h, Ar), pyrolysis (600 °C 2 h, Ar)	0.40 g L ⁻¹ (1.3 mM)	BPA (87.60 μM, 20 mg L ⁻¹)	¹ O ₂ -based degradation	6.5	1.04E-01	5.2	[7]
Fe _{SA} -N-C-20 (0.15)	Fe(NO ₃) ₃ ·9H ₂ O, Zn(NO ₃) ₂ ·6H ₂ O, 2-methylimidazole, methanol	Precursor synthesis (60 °C, 24 h), pyrolysis (900 °C 2 h, Ar)	0.40 g L ⁻¹ (1.3 mM)	BPA (87.60 μM, 20 mg L ⁻¹)	High-valent iron-oxo-based degradation	6.5	2.40E-01	1.6	[8]
SA-Cu/rGO (0.1)	Graphene oxide, sodium copper chlorophyllin, urea, ethanol	Precursor synthesis (60 °C), pyrolysis (550 °C 2 h and 700 °C 1 h, N ₂)	0.40 g L ⁻¹ (1.3 mM)	SMX (39.48 μM, 10 mg L ⁻¹)	[•] OH, SO ₄ ^{•-} and ¹ O ₂ -based degradation	6	8.76E-02	0.876	[9]
FeCo-NC (0.1)	FeCl ₂ ·4H ₂ O, CoCl ₂ ·6H ₂ O, poly(vinylpyrrolidone), K ₃ [Co(CN) ₆]	Precursor synthesis (60 °C 20 h), pyrolysis (500 – 800 °C 1 h, N ₂), acid washing (80 °C 4 h)	0.20 g L ⁻¹ (0.65 mM)	BPA (87.60 μM, 20 mg L ⁻¹)	¹ O ₂ -based degradation	6	1.25E+00	12.5	[10]

Mn-ISAs@CN	Mn(acac) ₃ , Zn(NO ₃) ₂ ·6H ₂ O, 2-methylimidazole, N, N-dimethylformamide, methanol	Precursor synthesis (120 °C, 5 h) and pyrolysis (900 °C 3 h, Ar)	0.20 g L ⁻¹ (0.65 mM)	BPA (87.60 μM, 20 mg L ⁻¹)	*OH and SO ₄ ^{•-} -based degradation	6	1.14E+00	5.7	[11]
Co-N-CNTs (0.1)	2,2-bipyridine, Co(acac) ₃ , CNTs	Precursor synthesis (60 °C), pyrolysis (800 °C 2 h, Ar), acid washing (70 °C 8 h)	1 mM	SMX (39.48 μM, 10 mg L ⁻¹)	Electron transfer-based degradation	6.8	1.57E-01	1.57	[12]
PCN-0.5 (0.05)	Dicyandiamide, polydopamine, dopamine	g-C ₃ N ₄ synthesis (550 °C, 4 h), precursor synthesis (60 °C, 12 h), pyrolysis (800 °C 2 h, Air)	1 mM	4-CP (155.57 μM, 20 mg L ⁻¹)	Electron transfer-based degradation	6.81	1.45E+00	29	[13]
NCN-900 (0.1)	Urea, glucose	g-C ₃ N ₄ synthesis (550 °C, 4 h), precursor synthesis (140 °C overnight), pyrolysis (900 °C 1 h, Air)	2 mM	BPA (100 μM)	¹ O ₂ -based degradation	6.7	3.1E+00	31	[14]
Co _{1.1} Mn _{1.9} O ₄ (0.05)	Co(NO ₃) ₂ ·6H ₂ O, (NH ₂) ₂ CO, NH ₄ F, MnCl ₂ ·4H ₂ O	Precursor synthesis (hydrothermal and refluxing), and pyrolysis (450 °C 1.5 h, Air)	0.1 g L ⁻¹ (0.325 mM)	SA (58.07 μM, 10 mg/L)	SO ₄ ^{•-} -based degradation	6.3	4.50E-01	9	[15]
Yolk-shell Co/C nanoreactors (0.1)	2-methylimidazole, Co(NO ₃) ₂ ·6H ₂ O, tannic acid	Precursor synthesis and pyrolysis (600 °C, N ₂)	0.15 g L ⁻¹ (0.488 mM)	BPA (87.6 μM, 20 mg L ⁻¹)	SO ₄ ^{•-} -based degradation	8.23	3.20E-01	3.20	[16]
3.0QS-CoS (0.2)	Pluronic P123, tetraethylorthosilicate, Co(NO ₃) ₂ ·6H ₂ O	Precursor synthesis (100 °C, 24 h), and pyrolysis (500 °C 5 h, Air)	2 g L ⁻¹ (6.5 mM)	Phenol (212.5 μM, 20 mg L ⁻¹)	SO ₄ ^{•-} -based degradation	-	3.20E-01	1.6	[17]

† Notes: AO7, orange acid II; 2-CP, 2-chlorophenol; BPA, bisphenol A; BPB, butyl paraben; CIP, ciprofloxacin; 4-CP, 4-chlorophenol; SA, sulfanilamide; SMX, sulfamethoxazole

Table S2. Reactivities of CNTs, N-CNTs, CoN_x-CNTs, Co₃O₄ and MnO₂ toward the activation of PMS (0.20 g L⁻¹) for oxidizing AO7 and other ROCs under different conditions.

Catalysts (mg L ⁻¹)	Pollutants ‡ (10 mg L ⁻¹)	Experimental conditions	Initial pH	Final pH	Released Co ions (mg L ⁻¹)	Degradation efficiency (% reaction time)	First-order reaction rate (min ⁻¹)	R ²
CNTs (50)	AO7	No ions	7.00	3.54	ND	58.62 (120 min)	8.61E-03 ± 1.34E-03	0.7695
N-CNTs (25)	AO7	No ions	7.00	3.46	ND	92.19 (30 min)	7.29E-02 ± 3.68E-04	0.9929
CoN _x (25)	AO7	No ions	7.00	3.38	ND	50.97 (30 min)	2.44E-02 ± 4.03E-03	0.9911
CoN _x -CNTs (25)	AO7	No ions	7.00	3.35	9.50E-02	98.24 (7.5 min)	9.29E-01 ± 1.92E-01	0.9943
cn-Co ₃ O ₄ (150)	AO7	No ions	7.00	3.52	1.70E-02	94.76 (120 min)	2.34E-02 ± 8.34E-03	0.9290
β-MnO ₂ (50)	AO7	No ions	7.00	3.52	ND	94.35 (120 min)	2.49E-02 ± 6.68E-03	0.9988
cn-Fe ₃ O ₄ (50)	AO7	No ions	7.00	3.64	ND	29.16 (120 min)	2.73E-03 ± 1.33E-04	0.9583
CoN _x -CNTs (25)	AO7	No ions	3.00	2.82	1.45E-01	98.26 (7.5 min)	6.52E-01 ± 1.73E-01	0.9942
CoN _x -CNTs (25)	AO7	No ions	5.00	3.24	1.07E-01	99.28 (7.5 min)	6.47E-01 ± 2.70E-02	0.9956
CoN _x -CNTs (25)	AO7	No ions	9.00	3.45	9.50E-02	98.07 (7.5 min)	6.68E-01 ± 1.64E-02	0.9974
CoN _x -CNTs (25)	AO7	No ions	10.60	6.72	7.30E-02	97.99 (7.5 min)	9.28E-01 ± 7.39E-02	0.9955
CoN _x -CNTs (25)	AO7	10 mM Cl ⁻	7.00	3.54	6.20E-02	93.02 (7.5 min)	7.32E-01 ± 1.44E-01	0.9964
CoN _x -CNTs (25)	AO7	10 mM NO ₃ ⁻	7.00	3.50	6.30E-02	93.85 (7.5 min)	7.77E-01 ± 9.15E-02	0.9778
CoN _x -CNTs (25)	AO7	10 mM HCO ₃ ⁻	7.00	8.06	5.30E-02	95.29 (7.5 min)	8.74E-01 ± 9.08E-03	0.9965
CoN _x -CNTs (25)	AO7	10 mM SO ₄ ²⁻	7.00	3.60	5.90E-02	94.47 (7.5 min)	8.45E-01 ± 1.79E-01	0.9972
CoN _x -CNTs (25)	AO7	10 mM PO ₄ ³⁻	7.00	6.90	3.50E-02	99.12 (7.5 min)	1.07E+00 ± 2.93E-02	0.9959
CoN _x -CNTs (37.5)	Phenol	No ions	7.00	3.27	1.24E-01	94.38 (20 min)	3.52E-01 ± 9.08E-02	0.9574
CoN _x -CNTs (37.5)	2-CP	No ions	7.00	3.34	8.01E-01	97.53 (5 min)	7.78E-01 ± 3.23E-02	0.9912
CoN _x -CNTs (37.5)	BPB	No ions	7.00	3.39	1.18E-01	98.40 (20 min)	3.25E-01 ± 3.95E-03	0.9760
CoN _x -CNTs (37.5)	BPA	No ions	7.00	3.24	1.00E-01	97.48 (20 min)	2.98E-01 ± 1.66E-02	0.9691
CoN _x -CNTs (25)	AO7	Tap water	6.80	4.44	5.50E-02	98.55 (5 min)	1.12E+00 ± 1.87E-01	0.9995
CoN _x -CNTs (25)	AO7	River water	7.90	6.84	5.50E-02	96.25 (5 min)	7.21E-01 ± 7.06E-02	0.9980

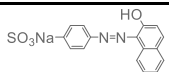
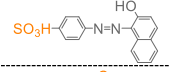
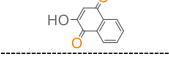
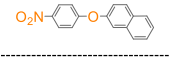
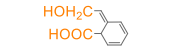

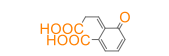
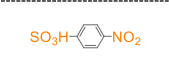
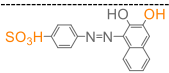
‡ Notes: AO7, orange acid II; 2-CP, 2-chlorophenol; BPA, bisphenol A; BPB, butyl paraben. ND means that the data were not available/detected.

Table S3. The analytic methods for detecting phenol, 2-CP, BuP and BPA using HPLC.

Types of ROCs	Detecting wavelength (nm)	Mobile phase †(A:M:UW, V:V:V)	Injection volume (μL)	Retention time (min)	Flow rate (mL min ⁻¹)
Phenol	270	10:50:40	50	3.85	1
2-CP	274	20:50:30	50	3.87	1
BuP	254	55:0:45	25	6.84	1
BPA	226	30:40:30	50	4.40	1

† Note: A and M stand for acetonitrile and methanol with chromatographic grade, respectively, while UW is short for ultrapure water (18.25 MΩ cm).

Table S4. Summary on the proposed oxidation products of AO7 by CoN_x-CNTs/PMS and their developmental toxicity and oral rate LD50.

Product Index	Detected m/z	Retention time (min)	Formula structure	Theoretical m/z	Molecular weight	Chemical formula	Proportion of products (%) [‡]	Developmental toxicity	Oral Rat LD50 (mg/kg)
AO7	-	-		350.0337	350.3237	C ₁₆ H ₁₁ N ₂ NaO ₄ S	0	0.98	8168.36
P328	327.04 (-MS model)	16.07		328.0518	328.3420	C ₁₆ H ₁₂ N ₂ O ₄ S	0.79	1.02	6486.34
P174	173.02 (-MS model)	10.58		174.0317	174.1550	C ₁₀ H ₆ O ₃	9.74	0.64	584.24
P265	266.08 (+MS model)	10.06		265.0739	265.2680	C ₁₆ H ₁₁ NO ₃	0.09	0.77	1363.65
P166	165.02 (-MS model)	8.79		166.0630	166.1760	C ₉ H ₁₀ O ₃	2.35	0.42	3495.63
P194	193.05 (-MS model)	10.76		194.0579	194.1860	C ₁₀ H ₁₀ O ₄	0.94	0.51	2371.47
P208	206.98 (-MS model)	11.18		208.0372	208.1690	C ₁₀ H ₈ O ₅	0.26	0.46	668.62
P202	203.07 (+MS model)	11.80		202.9888	203.1680	C ₆ H ₅ NO ₅ S	84.88	0.51	2734.26
P344	343.04 (-MS model)	12.72		344.0467	344.3410	C ₁₆ H ₁₂ N ₂ O ₅ S	0.96	0.83	6156.6

[‡] **Notes:** The ratios of the degradation products of AO7 by CoN_x-CNTs/PMS were calculated based on the peak area for each final product.

Author Contributions

Jia-Cheng E. Yang: Conceptualization, Methodology, Data curation, Writing-Original draft, Writing-Reviewing and Editing, and Funding acquisition.

Min-Ping Zhu: Methodology, Investigation, Data curation, and Formal analysis.

Darren Delai Sun: Writing-Reviewing and Editing.

Ming-Lai Fu: Supervision, Resources, Funding acquisition, and Writing-Reviewing and Editing.

Yu-Ming Zheng: Supervision, Resources, Funding acquisition, and Writing-Reviewing and Editing.

Notes and references

- [1] G. Zhang, Y. Jia, C. Zhang, X. Xiong, K. Sun, R. Chen, W. Chen, Y. Kuang, L. Zheng, H. Tang, W. Liu, J. Liu, X. Sun, W. Lin, H. Dai, *Energ. Environ. Sci.*, 2019, **12**, 1317-1325.
- [2] H. Sun, C. Kwan, A. Suvorova, H.M. Ang, M.O. Tadó, S. Wang, *Appl. Catal. B: Environ.*, 2014, **154 – 155**, 134-141.
- [3] H. Sun, Y. Wang, S. Liu, L. Ge, L. Wang, Z. Zhu, S. Wang, *Chem. Commun.*, 2013, **49**, 9914.
- [4] Z. Yang, J. Qian, C. Shan, H. Li, Y. Yin, B. Pan, *Environ. Sci. Technol.*, 2021, **55**, 14494-14514.

- [5] X. Mi, P. Wang, S. Xu, L. Su, H. Zhong, H. Wang, Y. Li, S. Zhan, *Angew. Chem. Inter. Edit.*, 2021, **60**, 4588-4593.
- [6] L.S. Zhang, X.H. Jiang, Z.A. Zhong, L. Tian, Q. Sun, Y.T. Cui, X. Lu, J.P. Zou, S.L. Luo, *Angew. Chem. Inter. Edit.*, 2021, **60**, 21751-21755.
- [7] Y. Gao, T. Wu, C. Yang, C. Ma, Z. Zhao, Z. Wu, S. Cao, W. Geng, Y. Wang, Y. Yao, Y. Zhang, C. Cheng, *Angew. Chem. Inter. Edit.*, 2021, doi: 10.1002/anie.202109530.
- [8] Y. Li, T. Yang, S. Qiu, W. Lin, J. Yan, S. Fan, Q. Zhou, *Chem. Eng. J.*, 2020, **389**, 124382.
- [9] F. Chen, X. Wu, L. Yang, C. Chen, H. Lin, J. Chen, *Chem. Eng. J.*, 2020, **394**, 124904.
- [10] X. Li, X. Huang, S. Xi, S. Miao, J. Ding, W. Cai, S. Liu, X. Yang, H. Yang, J. Gao, J. Wang, Y. Huang, T. Zhang, B. Liu, *J. Am. Chem. Soc.*, 2018, **140**, 12469-12475.
- [11] J. Yang, D. Zeng, Q. Zhang, R. Cui, M. Hassan, L. Dong, J. Li, Y. He, *Appl. Catal. B: Environ.*, 2020, **279**, 119363.
- [12] J. Miao, Y. Zhu, J. Lang, J. Zhang, S. Cheng, B. Zhou, L. Zhang, P.J.J. Alvarez, M. Long, *ACS Catal.*, 2021, 9569-9577.
- [13] J. Miao, W. Geng, P.J.J. Alvarez, M. Long, *Environ. Sci. Technol.*, 2020, **54**, 8473-8481.
- [14] Y. Gao, Z. Chen, Y. Zhu, T. Li, C. Hu, *Environ. Sci. Technol.*, 2019, **54**, 1232-1241.
- [15] Z.Y. Guo, C.X. Li, M. Gao, X. Han, Y.J. Zhang, W.J. Zhang, W.W. Li, *Angew. Chem. Inter. Edit.*, 2021, **60**, 274-280.
- [16] M. Zhang, C. Xiao, X. Yan, S. Chen, C. Wang, R. Luo, J. Qi, X. Sun, L. Wang, J. Li, *Environ. Sci. Technol.*, 2020.
- [17] Y. Yin, H. Wu, L. Shi, J. Zhang, X. Xu, H. Zhang, S. Wang, M. Sillanpää, H. Sun, *Environ. Sci.: Nano*, 2018, **5**, 2842-2852.